복사열손실이 있는 비예혼합 튜브형 화염의 화염셀 거동에 대한 수치 해석적 연구

박현수* · 유춘상*†

A Numerical Study of the Flame Cell Dynamics in Opposed Nonpremixed Tubular Flames with Radiative Heat Loss

Hyun Su Bak*, Chun Sang Yoo*†

ABSTRACT

The effects of radiative heat loss on opposed nonpremixed tubular flames are investigated by 2-D direct numerical simulations with linear stability analysis. The temperature response curve are obtained using finite difference method with a simple continuation method. The cellular instability by radiative heat loss is observed by 2-D simulations using different initial conditions. Three different oscillation modes of the flame are observed prior to the onset of cellular instability: decaying, stable and amplified oscillation of temperature. Propagating and rotating flame cells are also found at extremely large Damköhler number beyond the radiation-induced extinction limit. The displacement speed analysis reveals the characteristics of the flame cell dynamics in opposed nonpremixed tubular flames with radiative heat loss.

Key Words : Opposed nonpremixed tubular flame, Cellular instability, Radiation heat loss, Propagating and rotating flame, Displacement speed analysis

The diffusive-thermal instability of nonpremixed flames with their effective Lewis number being less than unity near the transport-induced extinction has been extensively investigated by experiments and numerical studies [1-6]. The characteristics of flame instabilities in various burner configurations including an axisymmetric jet, a Wolfhard-Parker, a counterflow burner, and a tubular flame burner have been investigated. Especially, tubular flames have an inherent advantage that the stretch rate and curvature can be independently specified due to the tubular shape, and hence, many parametric studies have been conducted to understand the effects of stretch rate and curvature on the diffusive-thermal instability [1-4]. Through a numerical study using 2-D simulations and linear stability analysis, it was recently found that it is possible to predict the flame cell characteristics such as the number of flame cells, the critical Damköhler number, Da_C, the onset of the cellularity with good accuracy [6]. Even though there have been many studies on the cellular instability near the transport-induced extinction limit, there have been few studies on those with radiative heat loss.

In general, when the radiative heat loss exists in flames, it is widely known that two extinction Damköhler numbers, Da_E, exist on both sides of the temperature response curve: i.e. the transport-induced extinction and radiation-induced extinction. The cellular and oscillatory instabilities are especially found near the radiation-induced extinction. Three types of flame-evolution such as decaying oscillatory solution, diverging solution to extinction, and stable limit-cycle solution are shown from nonlinear dynamics of diffusion flame oscillations with radiative heat loss and unity Lewis numbers for all species [7]. The characteristics of radiative diffusion flames with the Lewis number of fuel being less than

* 울산과학기술원 기계공학과
† 연락저자, csyoo@unist.ac.kr
TEL : (052)217-2322 FAX : (052)217-2409

unity in 2-D plane counterflow configuration were investigated by 2-D simulations using various initial profiles based 1-D analysis [8]. Different flames such as a wavy flame, a stationary cellular flame, and a propagating cellular flame were found.

In present study, the effects of radiative heat loss on opposed nonpremixed tubular flames are investigated using 2-D direct numerical simulations with linear stability analysis. Prior to performing 2-D simulations of opposed nonpremixed tubular flames with radiative heat loss, the characteristics of 1-D steady tubular flames are investigated to specify the radiation-induced extinction Damköhler number, $Da_{R,E}$. By assuming no radiation effect on the mass fraction of all species, non-dimensional governing equations are given as follows:

$$u_r \frac{d}{dr}\begin{pmatrix} T \\ Y_F \\ Y_O \end{pmatrix} = \frac{1}{r}\frac{d}{dr}\left(r\frac{d}{dr}\right)\begin{pmatrix} T \\ Y_F/L_F \\ Y_O/L_O \end{pmatrix} + Da\, Y_F Y_O e^{-T_a/T}\begin{pmatrix} q \\ -\alpha_F \widetilde{Y_{O2}} \\ -\alpha_O \widetilde{Y_{F,1}} \end{pmatrix} - Ra\begin{pmatrix} T^4 - T_\infty^4 \\ 0 \\ 0 \end{pmatrix} \quad (1)$$

where T, Y_F, and Y_O are the non-dimensional temperature, fuel and oxidizer mass fractions, respectively. Ra $(=4\sigma \widetilde{T_{ref}^3} pK/\tilde{\rho}\tilde{c}_p\tilde{\kappa})$ is a constant radiation-induced parameter related to radiative heat loss, where Stefan-Boltzmann constant, σ, partial pressure, p, Planck mean absorption constant, K, etc. are used for normalization. Although K is a property depending on temperature and species, it can be considered as a function of Da only because it has little effect on the instability of heat and mass transfer [7]. In present study, $Ra = I \times Da$ where the intensity of the radiation, $I = 10^{-8}$, is adopted for the simplification of the analysis. For more details of other variables and constants, readers can refer to Ref. [6].

Equation (1) is solved by the Newton-Raphson method with a simple continuation method to obtain a temperature response curve. 2-D direct numerical simulations with various initial conditions based on 1-D solutions are performed using eight-order finite difference scheme spacially and fourth-order explicit Runge-Kutta method for time integration [6].

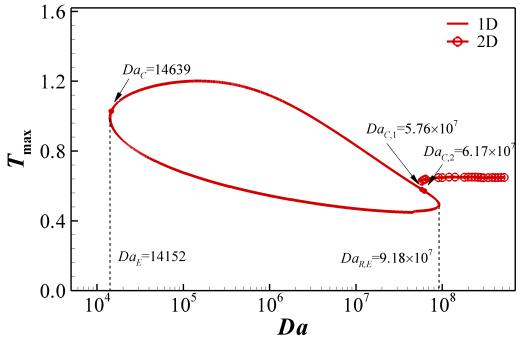

Fig. 1 The maximum flame temperature, T_{max}, as functions of the Damköhler number, Da. Solid line and circles represent T_{max} of 1-D and 2-D solutions using the perturbed initial condition, respectivly.

Figure 1 shows the maximum flame temperature, T_{max}, as a function of Damköhler number, Da. Near the transport-induced extinction limit, the response curve of T_{max} is quite similar to that without radiative heat loss in [6]. Near the radiation-induced extinction limit, however, T_{max} decreases with increasing due to the radiative heat loss.

The perturbed initial condition is used to investigate the cellular instability of opposed nonpremixed tubular flames near $Da_{R,E}$. The cellular instability by radiative heat loss first occurs at Da = 5.80×10^7, and the number of flame cells, N_{cell}, is 29. These are approximately similar to the results of the linear stability analysis where $Da_{C,1}$ = 5.76×10^7 and the maximum wavenumber of the highest growth rate, k_{max} = 28.6. As Da increases, N_{cell} decreases from 29 to 25 at Da = 6.20×10^7. It is also similar to the second critical Damköhler number that the real part of the complex growth rate becomes positive, $Da_{C,2}$ = 6.17×10^7. From the results, it can be concluded that near the radiation-induced extinction limit, the linear stability analysis can also predict the critical Damköhler number and N_{cell} with reasonable accuracy.

In terms of oscillation, the tubular flames between two critical Da exhibit a feature that the flame oscillation is decayed from the beginning of simulations. At $Da_{C,2}$, the flame oscillation prior to the onset of the cellular

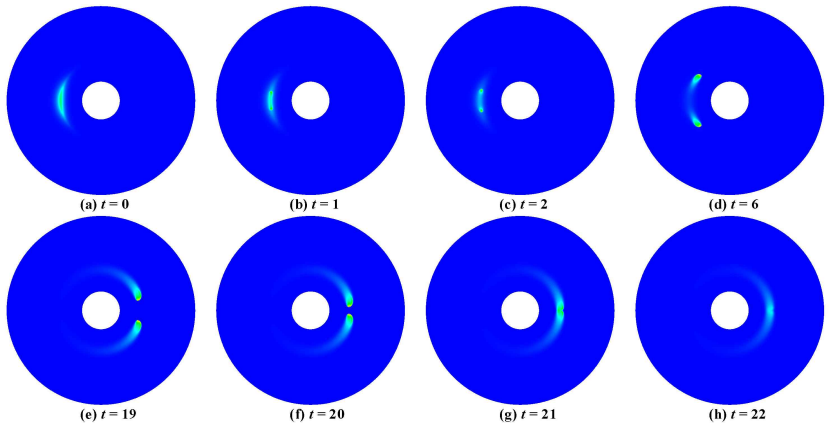

Fig. 2 Temporal evolution of the temperature isocontours using the C-shaped initial condition, Da = 5.00×10^{8}

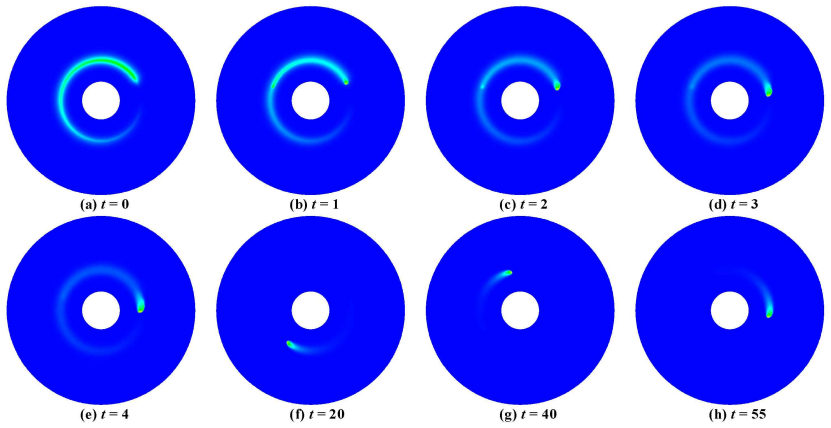

Fig. 3 Temporal evolution of the temperature isocontours using the artificially asymmetry initial condition, Da = 5.00×10^{8}

instability is stable. Beyond $Da_{C,2}$, however, the oscillation is gradually amplified and cellular flame instability occurs at Da = 6.20×10^{7} near $Da_{C,2.}$ In this case, the cellular flames survive although T_{max} is amplified from the onset of the simulation.

With the previous solution from Da = 5.80×10^{7}, Da is gradually increased to find the total extinction of the flame. The total radiation-induced extinction Da is approximately 5.20×10^{8}. N_{cell} and T_{max} are maintained, and the cell size is reduced. These are analogous to the results near transport-induced extinction.

The 2-D simulations using the C-shaped initial condition at extremely large Da beyond $Da_{R,E}$ are performed to generate propagating flames by strong radiative heat loss. For instance, the Da of the tubular flame initialized $Da_{C,2}$ = 6.17×10^{7} is radically increased to Da = 5.00×10^{8}. Figure 2 shows the temporal evolution of the temperature isocontours using the C-shaped initial condition. Initial C-shaped area is kept small to minimize the effects of initial condition. Under very large radiative heat loss conditions, the flame develops into two flame cells propagating towards each other (a)~(d) and then, flame extinction occurs when two flame cells collide each other (e)~(h).

By adopting the artificially asymmetric initial conditions, a rotating flame cell is found at the same Da. Figure 3 shows the temporal evolution of temperature using the asymmetric

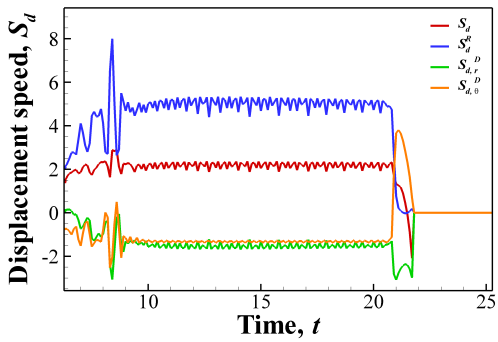

Fig. 4 The displacement speed, S_d, of only one flame cell and components of it as functions of time, t, in case of the propagating flame at $Da = 5.00\times10^{8}$.

initial condition. At $Da = 5.00\times10^{8}$, only one flame cell survives (see Fig. 3(a)~(e)) and then, it keeps rotating clockwise (see Fig. 3(f)~(h)).

The displacement speed, S_d, analysis is conducted to identify the dynamics of the propagating flames. For the details of the analysis, readers can refer to Ref. [6]. S_d is evaluated at $Y_F = 0.06065$ along the stagnation plane. It is found that the propagating and rotating flame cells consist of a leading zone featuring positive S_d and a backward zone having negative S_d because of the radiative heat loss.

Figure 4 shows the temporal evolution of the displacement speed, S_d, of a flame cell and its components originated from the C-shaped initial conditions at $Da = 5.00\times10^{8}$. In this case, the flame oscillation occurs from the beginning of the simulation to the total extinction by the collision of each flame cell. During the early phase of evolution, S_d oscillates significantly due to the rapid change of flame shape by radiative heat loss. After transient region, S_d remains stable. When the collision between two flame cells occurs, S_d is rapidly decreased due to the reduction of reaction.

Acknowledgements

This work was supported by the Space Core Technology Development Program (NRF-2015M1A3A3A02027319) through the National Research Foundation of Korea grant funded by the Ministry of Science, ICT and Future Planning. This research used the resources of the UNIST Supercomputing Center.

References

[1] S. Hu, P. Wang, R. W. Pitz, *Proc. Combust. Inst.* 31, 2007, pp 1093-1099.
[2] S. Hu, R. W. Pitz, *Combust. Flame* 156, 2009, pp 51-61.
[3] S. Hu, R. W. Pitz, Y. Wang, *Combust. Flame* 156, 2009, pp 90-98.
[4] S. W. Shopoff, P. Wang, R. W. Pitz, *Combust. Flame* 158, 2011, pp 876-884.
[5] M. Short, J. Buckmaster, S. Kochevets, *Combust. Flame* 125, 2001, pp 893-905.
[6] H. S. Bak, S. R. Lee, J. H. Chen, C. S. Yoo, *Combust. Flame* 162, 2015, pp 4612-4621.
[7] C. H. Sohn, J. S. Kim, S. H. Chung, K. Maruta, Combust. Flame, 123, 2000, pp 95-106.
[8] J. R. Nanduri, C. J. Sung, J. S. T'len, Combust. Theory Model., 9, 2005, pp 515-548.